THE JOURNAL OF PHYSICAL CHEMISTRY B

Article

pubs.acs.org/JPCB

Investigation of Poly(lactide) Stereocomplexes: 3-Armed Poly(L-lactide) Blended with Linear and 3-Armed Enantiomers

Jun Shao,[†,‡] Jingru Sun,[†] Xinchao Bian,[†] Yi Cui,[†] Gao Li,*[,†] and Xuesi Chen*[,†]

[†]Key Laboratory of Polymer Ecomaterials, Changchun Institute of Applied Chemistry, Chinese Academy of Sciences, Changchun 130022, China

[‡]Graduate University of the Chinese Academy of Sciences, Beijing 100039, China

ABSTRACT: Stereocomplex poly(lactide)s (sc-PLAs) were obtained from solution blending of 3-armed poly(L-lactide) (3PLLA) and linear poly(D-lactide) (PDLA) and between enantiomeric 3PLAs. Differential scanning calorimetry and wide-angle X-ray diffraction results indicated that racemic crystallites were preferentially produced in all the binary blends. The melting temperature and fusion enthalpy of racemic crystallites were remarkably different through varying the structure, constituent, and molecular weight of PLA. Through this investigation, higher melting temperatures were obtained in the middle molecular weight binary blends, and the highest melt temperature of racemic crystallites reached to 246 °C, it was the highest reported value until now. In similar molecular weight blends (or the linear PLA was similar to each branch of 3PLA enantiomers), with the composition of 3PLA increasing, the phase separation molecular weight decreased gradually ($M_{\text{linear/linear blends}} > M_{\text{linear/3-armed blends}} > M_{\text{3-armed/3-armed blends}}$). The structure distinction between 3PLA and linear PLA induced different thermal properties and phase behaviors of the 3PLLA/PDLA and 3PLLA/3PDLA blends. The thermal properties of these mixtures and its variations provided basic data for their industrial applications.

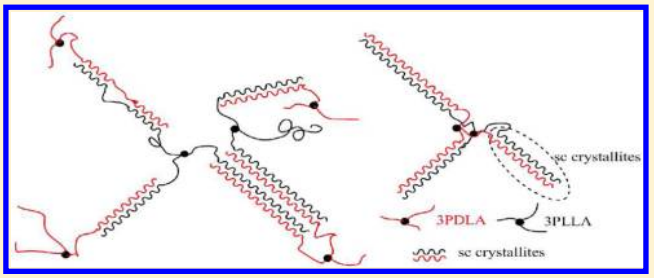

1. INTRODUCTION

Biodegradable polyesters are mainly utilized materials for biomedicine, tissue scaffold, and environmental applications because of their biodegradability, low toxicity, biocompatibility, and good mechanical performances.[1] Poly(lactide) (PLA) can be derived from nature resources, such as corn starch and sugar beets, via fermentation,[2] and its products are degradable under natural circumstances.[3,4] Most importantly, parts of the mechanical properties of PLA can compared favorably with polypropylene (PP), polyethylene (PE), and polystyrene (PS), which were three widely used general-purpose plastics.[5] These excellent properties made PLA to be widely concerned in recent years.[1,6] In 1987, Ikada et al. found the stereocomplex crystallites, formed after poly(L-lactide) (PLLA) blended with poly(D-lactide) (PDLA), whose melting temperature was 50 °C higher than neat PLA.[7] Since this first report, intensive studies had been focused on the stereocomplex poly(lactide) in a short time because of its higher thermal performances and potential wider applications.[8−12] Until now, most of research works has been investigated on the mechanical and thermal properties of PLLA/PDLA blends,[13−19] different molecular weight blends,[9,20,21] different L/D ratio blends,[22−25] morphology,[26−28] self-assembly of polylactide stereocomplexes,[29] and PLA block copolymers,[30−40] etc. However, few researchers paid attention to the stereocomplexation between multiarmed PLA and linear enantiomers and between enantiomeric multiarmed PLAs. Nowadays, more focus has been on the multiarmed or hyperbranched polymers because of their particular topological structure and interesting physical/chemical properties.[41−43] Biela et al. have done lots of creative investigations on multiarmed PLA[44−47] and multiarmed PLA enantiomeric blends,[48,49] and they found that when high molecular weight of star-shaped PLA (300 kg/mol, for example) was blended with its enantiomers, if the branches of the star-shaped PLA reached 13 or more, only stereocomplexes were formed in the blends. However, the average molecular weight of each branch of these star-shaped PLAs was not more than 30 kg/mol. Besides, some researchers studied the synthesis and physicochemical properties of the stereocomplex biodegradable hydrogels,[50,51] and other research groups investigated the crystallization and physical properties of linear PLA and multiarmed PLA.[52,53] Notwithstanding, lots of issues on the blends of multiarmed PLAs were still unknown, for example, what will happen if multiarmed PLA blended with linear enantiomers; whether there was a molecular weight and stereocomplex crystallites predominately formed between enantiomeric multiarmed PLA blends under that molecular weight.

In this paper, the stereocomplex crystallites were obtained by blending 3-armed poly(L-lactide) (3PLLA) with linear enantiomers at the first time, and the thermal properties and phase behaviors of these 3PLLA/PDLA blends were compared

Received: April 9, 2012
Revised: June 15, 2012
Published: July 31, 2012

to corresponding 3PLLA/3-armed PDLA (3PDLA) blends. Exploring the influences of different structure and composition of PLAs on the physical properties of the blends will provide the basis for its commercial application.

2. EXPERIMENTAL SECTION

Materials and Specimens Preparation. L-Lactide (L-LA) and D-lactide (D-LA) were purchased from Purac (optical purity ≥99.5%) and were purified by recrystallization from dry acetic ether. 3PLLA, PDLA, and 3PDLA were synthesized by the ring-opening polymerization of L-LA and D-LA as described in the literature.[54] Isopropanol and propanetriol were used as the initiator for linear PLA and 3-armed PLA, respectively. The synthesis routes of linear PDLA and 3PDLA are shown in Scheme 1. The synthesis and structure of 3PLLA were similar to 3PDLA, and its synthesis was omitted. The synthesized polymers were purified by repeated precipitation, and dichloromethane was used as solvent and methanol as the nonsolvent. The products were dried in vacuum at room temperature for a week and at 60 °C in vacuum for another week before used.

Scheme 1. Synthesis Routes of Linear PDLA and 3-Armed PDLA (3PDLA)

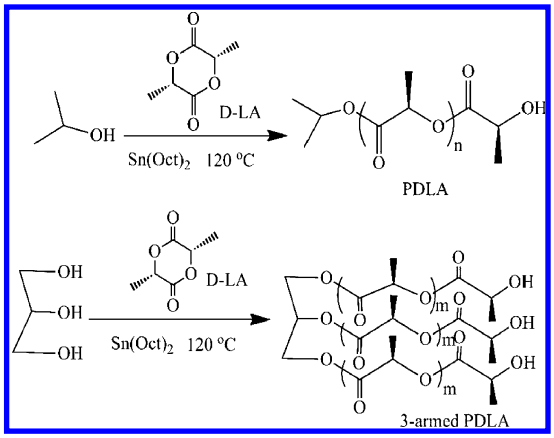

The numbers before and after PLA were coded as the branch of the PLA and number-average molecular weight, separately. Taking 3PDLA33 for example, it indicated that the number-average molecular mass of the 3-armed PDLA was 33 kg/mol. The number 1 was omitted before PDLA if it was linear PDLA. The molecular characteristics and melting temperatures of PLA utilized in this study are listed in Table 1.

The blending films used for physical measurements were prepared with the method described in the literature.[9] 3PLLA, PDLA, and 3PDLA were dissolved in dichloromethane separately, and the concentration of the solution was 1 g/dL. 3PLLA and PDLA (or 3PDLA) solution were admixed under vigorous stirring for 3 h; after that, the mixed solution was casted onto a Petri dish, followed by solvent evaporation at room temperature. The resulting films were dried in vacuum for a week at room temperature prior to physical measurements. The mixing L/D (weight) ratio of the blends was fixed at 1:1 if not mentioned otherwise. The 3PLLA35/PDLA32 or 3PLLA35/3PDLA33 different ratio blends, coded as 3PLLA35/PDLA32 *x*/*y* or 3PLLA35/PDLA33 *x*/*y*, where *x* and *y* represented the L and D ratio in the blend. If there was not number on the right, which indicated the L/D ratio was 1/1. The L ratio in the blends was calculated as follows:

Table 1. Molecular Characteristics and Melt Temperature of PLA

code	M_n (kg/mol)	M_w/M_n	T_m (°C)
3PLLA35	35	1.4	162.1
PDLA8	8	1.1	156.8
PDLA11	11	1.3	160.8
PDLA16	16	1.3	166.0
PDLA21	21	1.1	169.6
PDLA32	32	1.1	172.5
PDLA40	40	1.1	174.0
PDLA63	63	1.8	176.6
PDLA102	102	1.6	177.5
3PDLA9	9	1.1	145.8[a]
3PDLA33	33	1.1	163.9[b]
3PDLA57	57	1.4	170.8
3PDLA100	100	1.6	175.8
3PLLA10	10	1.4	150.2[c]
3PLLA60	60	1.4	171.5
3PLLA95	95	1.5	173.4
3PLLA130	130	1.3	175.1

[a]There was another minor melt peak at 154 °C. [b]3PLLA33 had two melt peaks during scanning: 159.7 °C (minor) and 163.9 °C (major). [c]A minor peak was found at 141 °C.

$$X_L = \frac{m(3PLLA)}{m(3PLLA) + m(PDLA)} \text{ or } X_L = \frac{m(3PLLA)}{m(3PLLA) + m(3PDLA)} \quad (1)$$

m referred to in the formula was the quality of each PLA separately.

Physical Measurements. The number- and weight-average molecular weights (M_n and M_w) of different polymers were evaluated in chloroform at 35 °C by using a Waters gel permeation chromatography (GPC) system with two Styragel HR gel columns (HR2 and HR4), and polystyrene was used as the standard. The GPC results of PLA and 3PLAs are listed in Table 1.

The thermal properties of neat PLAs and their binary blends were examined by differential scanning calorimeter (DSC) (DSC Q100, TA Instruments). To ensure reliability of the data obtained, heat flow and temperature were calibrated with standard indium (T_m = 156.6 °C and ΔH = 28.5 J/g). DSC scans were carried out at the speed of 10 °C/min from 20 to 250 °C under nitrogen atmosphere to investigate the crystallization behavior of the specimens (parts of specimens were heated to 260 °C for melting the specimens thoroughly). The first scan was recorded to compare the melting temperatures and fusion enthalpies of different samples. For pure PLA and 3PLA specimens, the DSC scans were performed from 20 to 200 °C at the speed of 10 °C/min.

The crystallinity of the stereocomplex (X_{sc}) was calculated as

$$X_{sc}\% = \frac{\Delta H_{sc}}{142\ \text{J/g}} \times 100\% \quad (2)$$

and the crystallinity of the homocrystal of PLA (X_{hm}) was calculated as

$$X_{hm}\% = \frac{\Delta H_{hm}}{93\ \text{J/g}} \quad (3)$$

dx.doi.org/10.1021/jp303402j | J. Phys. Chem. B 2012, 116, 9983−9991

The ΔH_{sc} (fusion enthalpy) was the value of the polylactide stereocomplex crystallites in the blend, which was calculated from the DSC measurement, and the 142 J/g was the reported enthalpy value for the crystals had infinite thickness for PLA stereocomplexes.[55] The ΔH_{hm} was referred to the fusion enthalpy value of the homochiral crystallites of PLA, and 93 J/g was the reported ΔH_m values for the 100% crystallized PLLA.[56] If there was an exothermic peak (which integral value was coded as ΔH_c) during the DSC scan, the ΔH_{hm} was calculated as

$$\Delta H_{hm} = \Delta H_m - \Delta H_c \quad (4)$$

ΔH_m is referred to the fusion enthalpy of the specimen during heating.

The wide-angle X-ray diffraction (WAXD) measurement was carried out on a Bruker D8 Advance X-ray diffractometer, using Cu Kα radiation; the scattering angle ranged from $2\theta = 10°$ to 30° at a scan speed of 3°/min at room temperature.

3. RESULTS AND DISCUSSION

3.1. Blended Polymers with Dissimilar Molecular Weights. *1.1. For the Blends of 3PLLA35/PDLA.* The DSC thermograms of 3PLLA35 blended with different molecular weights of PDLA are shown in Figure 1a. It was seen that only one endothermic peak was detected in all blending films, and the temperature of these peaks was higher than 180 °C, which implied that only stereocomplex crystallites formed in these blends. The crystallinity (X_{sc}) and melt temperature (T_{sc}) of stereocomplex calculated form Figure 1a are dotted in Figure 1b. The X_{sc} decreased with the increasing molecular weight of PDLA, which was due to the high motion ability of linear PDLA with relative low molecular weight, and it can penetrate deeply into the branch of 3PLLA. Thus, the stereocomplex crystallites could generate effectively. The T_{sc} first increased and then decreased as the molecular weight of PDLA increased from 8 to 102 kg/mol. The highest T_{sc} (230.7 °C) was found in the blend of 3PLLA35/PDLA16, which may associate with the length of PDLA chain was similar to the branch of 3PLLA35, and the thickness of stereocomplex crystal lamellae was highest.

Figure 2 describes the speculated mode of the stereocomplex formation between 3PLLA35 and dissimilar linear PDLA schematically. In the 3PLLA/PDLA (and also 3PLLA/3PDLA blends below mentioned), the branches of 3PLLA and PDLA chain (or the branch of 3PDLA) were packed side by side orderly to form the stereocomplex crystallites,[57] and the stereocomplexation can be done as the parallel and antiparallel formats.[48,49] Although Brizzolara et al. calculated the interaction energy of parallel structure in the linear PLLA/PDLA blends had more stable configuration (−119 kcal/mol),[58] the energy of the antiparallel format was slightly higher than that of parallel complexes (−111 kcal/mol). Both of these two formats were more stable than the 3_1-helix of PLLA (−96 kcal/mol), and the steric hindrance should be also enormous if the 3PLLA complexed with 3PDLA as the parallel format.

Compared to 3PDLA, the linear PDLA had the higher mobility, and it could complex with each branch of 3PLLA in the 3PLLA/PDLA blends. If the molecular weight of PDLA was lower than the branch of 3PLLA, the crystallites were more produced because of the high mobility of the PDLA. But stronger chain mobility also resulted in lower T_{sc} (3PLLA35/PDLA8). When the molecular weight of PDLA was approximate to the branch of 3PLLA, the length of the crystal period was longest and the T_{sc} was highest (3PLLA35/PDLA16). The stereocomplexes reduced if the molecular weight of PDLA continued increasing because the increasing entanglement and viscosity inhibited chain diffusing and complexation. The uncomplexed chain segment of PDLA and 3PLLA existed in the amorphous state in the blends, which made the crystallization to be difficult, conducted the depressing of the T_{sc} and X_{sc}. The variation of X_{sc} in the 3PLLA35/PDLA blends was similar to the reported linear PDLA/PLLA blends,[8,9] and the slight difference of the T_{sc}

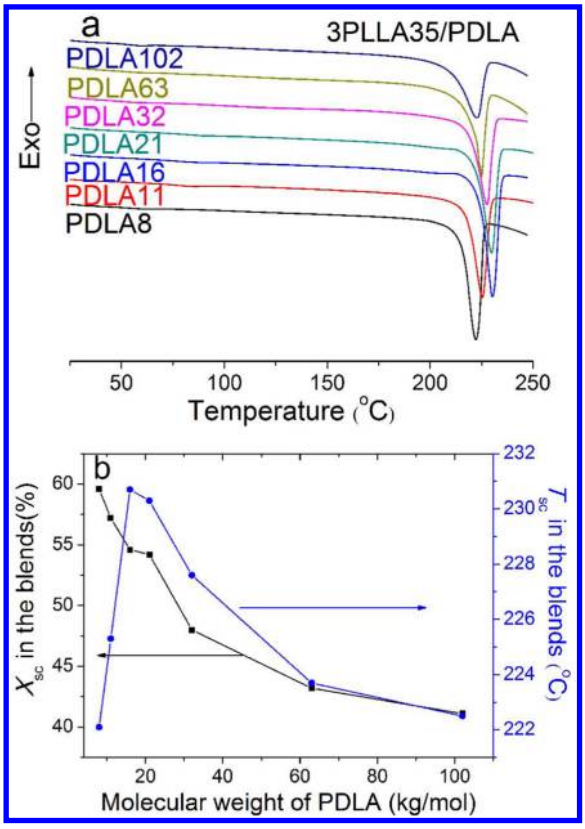

Figure 1. (a) DSC theromgram of 3PLLA35/PDLA blends with dissimilar molecular weight of PDLA. (b) Crystallinity (X_{sc}) and melt temperature (T_{sc}) of the 3PLLA/PDLA blends.

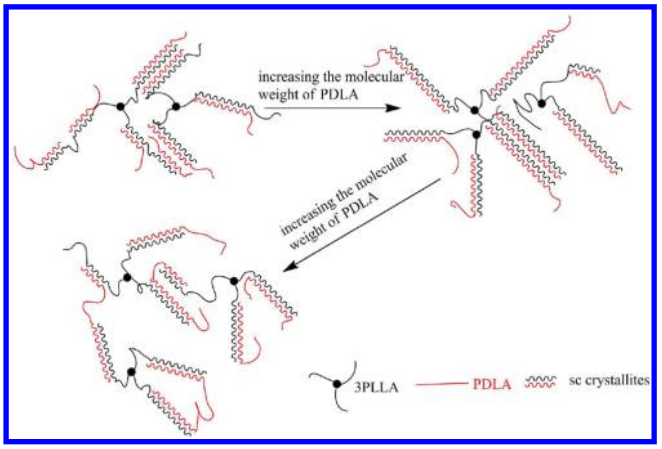

Figure 2. Speculated mode of the stereocomplex formation between 3PLLA35 and dissimilar linear PDLA.

dx.doi.org/10.1021/jp303402j | J. Phys. Chem. B 2012, 116, 9983−9991

variation may due to the different structure of 3-armed PLLA and linear PLLA.

1.2. For the Blends of 3PLLA35/3PDLA. In the 3PLLA35/dissimilar 3PDLA blending films (Figure 3a,b), both the T_{sc} and

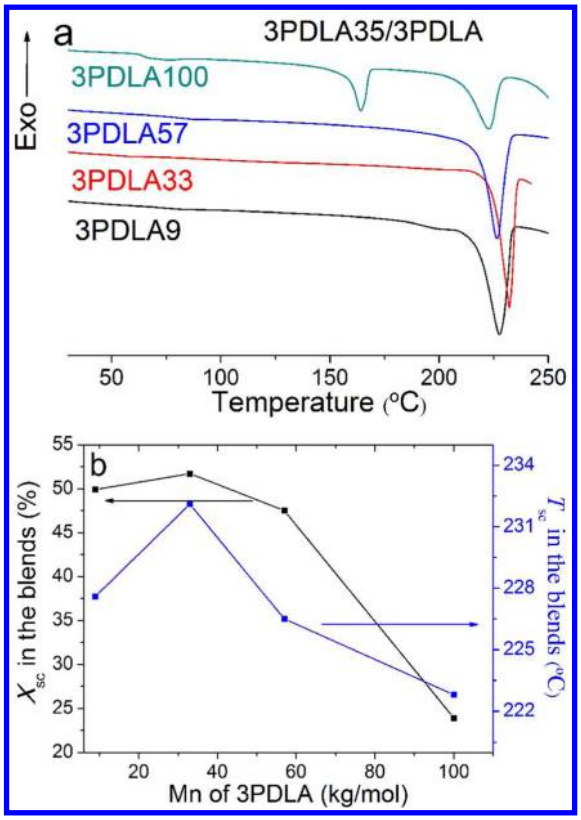

Figure 3. (a) DSC of 3PLLA35/3PDLA blends with dissimilar molecular weight of 3PDLA. (b) X_{sc} and T_{sc} of 3PLLA35/3PDLA blends.

X_{sc} increased at first and then depressed when the molecular weight of 3PDLA increased from 9 to 100 kg/mol. The T_{sc} and the X_{sc} were upmost when the molecular weight of 3PLLA and 3PDLA were ca. 35 kg/mol. Homochiral crystallites were observed as well as stereocomplexes after the molecular weight of 3PDLA reached to 100 kg/mol; it was clearly distinct from the above-mentioned 3PLLA35/PDLA blends. This phenomenon should be attributed to the larger steric hindrances from 3PLA, and it made the complexation become difficult; then the chains that did not participate in stereocomplexation congregated together and formed homocrystallites.

The possible complexation mode of 3PLLA35 with dissimilar 3PDLA is shown in Figure 4. When the molecular weight of 3PDLA was low (e.g., 9 kg/mol), the stereocomplexes would be easily formed due to the relative high motion ability. However, the branch was short, and the crystal period of the stereocomplexes was minor. Thus, the T_{sc} was not high. As the molecular weight increased (like 57 kg/mol or higher), the crystallizable chain segment of the branch increased; howbeit, the viscosity and entanglement of the polymer enhanced rapidly, and the interdiffusion of the polymer chain became difficult. Accordingly, the stereocomplexation was depressed. As a result, a balance existed among these contributing factors, and the T_{sc} was highest in the middle molecular weight blends, ca. 35 kg/mol.

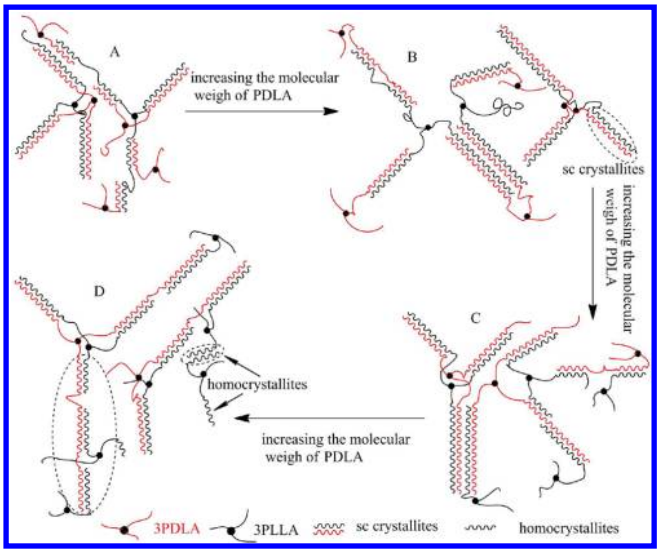

Figure 4. Speculated mode of the stereocomplexation between 3PLLA35 and dissimilar 3PDLA.

Homocrystal was found in the 3PLLA35/3PDLA100, and the melting temperature of homochiral crystal (T_{hm}) was 164 °C, similar to the melting temperature of 3PLLA35. The length of the branch in 3PDLA100 was almost 2 times longer than that in 3PLLA35. In theory, three branches of 3PLLA chain can complex with one branch of 3PDLA100 (as shown in the dashed cycle in Figure 4D). But it was implausible because of the huge steric hindrance from 3PDLA and repulsive effects among 3PLLAs for such compact arrangement. Therefore, parts of surplus 3PLLA chain did not involve in complexation, and they aggregated together and formed homochiral crystallites. Only stereocomplexes was formed in 3PLLA35/PDLA blends, which was due to the relative higher motion ability of linear PDLA. It could stereocomplex with 3PLLA35 easily. In addition, one PDLA chain can complex with more than one branch of 3PLLA35 at appropriate time, thus confining the congregation of PDLA and restraining the formation of homocrystallites.

2. Blended Films with Different L/D Ratios. Figure 5a displays the DSC curves of 3PLLA35/PDLA32 blended films with different L/D weight mixing ratios. An obvious exothermic peak was observed in neat 3PLLA specimen during DSC scanning, which implied the slow crystallization of 3PLLA during solution evaporating. However, there were no exothermal peak in the binary blends during heating, which could account for the preferentially formed racemic crystal could act as nuclei and accelerated the formation of homochiral crystal.[8,16,25] It was clear that the neat 3PLLA35 gave a single endothermic peak around 160 °C, whereas an additional peak was observed in the vicinity of 230 °C for the blending polymers. When the L ratio approached 0.5, the DSC peak around 160 °C became broader and finally vanished, while the peak around 230 °C remained and enhanced gradually. The T_{hm} and T_{sc} estimated from Figure 5a are plotted as a function of L weight ratio of the mixed polymers in Figure 5b. Apparently, T_{hm} decreased linearly as L ratio closing to 0.5, probably because the homopolymer crystallites became smaller and finally disappeared. And T_{sc} increased consecutively as the L ratio approached 0.5 because the crystallites of racemic became larger. The crystallinities of homopolymer crystallites (X_{hm}) and X_{sc} calculated from Figure 5a are shown in Figure 5c.

dx.doi.org/10.1021/jp303402j | J. Phys. Chem. B 2012, 116, 9983−9991

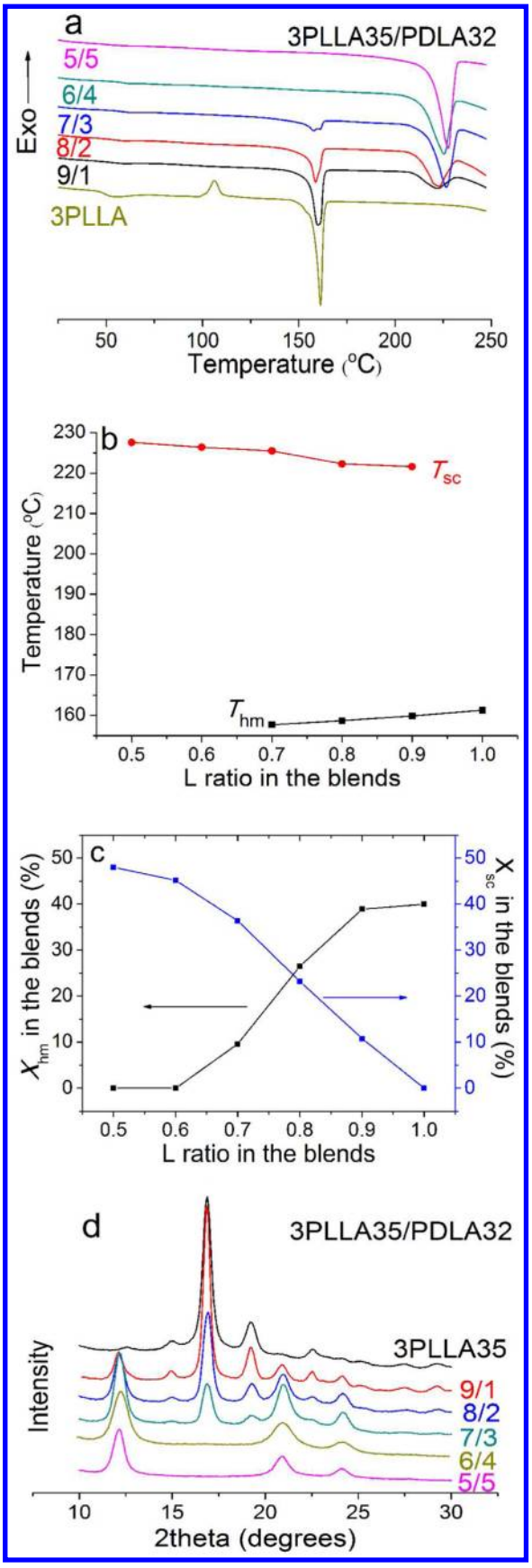

Figure 5. (a) DSC curves of 3PLLA35/PDLA32 with different L/D ratios. (b) T_{hm} and T_{sc} of the 3PLLA35/PDLA32 different ratio blends. (c) X_{hm} and X_{sc} of these blends. (d) WAXD profile of these blends.

The X_{hm} decreased while the X_{sc} increased continuously, respectively, as the L ratio decreased from 1 to 0.5. Although only the melt peak of stereocomplexes was detected when L ratio was 0.6, the melting temperature and fusion enthalpy of the racemic crystallites were the highest in equal weight blend. Thus, the most favorable L ratio for the formation of racemic crystallites was 0.5 in 3PLLA35/PLLA32 different ratio blends. These regularities were similar to linear PLLA/PDLA blends (M_n < 60 kg/mol).[7,8]

From the WAXD of the casted films (Figure 5d), it found that two most intense crystalline diffraction peaks were observed at 16.8° and 19.1° in pure 3PLLA film, which were respectively assigned to diffractions from the (110)/(200) and (203) planes for the α-form (or α'-form). The relatively low-intensity diffraction peaks at 14.8° and 22.4° specific to the α-form of PLA were also observed in the film,[59−61] which implied that the neat 3PLLA specimen crystallized in ordered α-form during solution evaporating. The diffraction peaks at 12°, 21°, and 24° belonging to PLA stereocomplex crystal were detected since the L ratio was 0.9;[7] the intensities of these peaks were enhanced as the L ratio decreasing to 0.5 in the blends, while the diffraction peaks assigned to 3PLLA homochiral crystal became weak at the same time and disappeared at last.

For 3PLLA35/3PDLA33 blends with different L ratios, the results in Figure 6a−c revealed the same regularities as 3PLLA35/PDLA32 blends. However, the results indicated that the T_{sc} and X_{sc} in 3PLLA35/3PDLA33 were higher than corresponding 3PLLA35/PDLA32 binary blends (compare Figure 5b to Figure 6b); the reinforcement of X_{sc} and the retreatment of X_{hm} in 3PLLA35/3PDLA33 blends were steeper when the L ratio was decreasing from 1 to 0.5 (Figures 5c and 6c). These results implied that the X_{sc} formed in the 3PLLA35/3PDLA33 blends were more sufficient and stable. These disparities may be assigned to the asymmetric structure between 3PLLA and linear PDLA, and the complexation was partially retarded. Figure 6d displays the WAXD of the 3PLLA35/3PDLA33 with different ratios. It was interesting to discover that the diffraction peak (16.8°) was still appeared when the L ratio was 0.6, which attested that homocrystallites were formed in that blend. This may due to the adequately complexation between 3PLLA and 3PDLA; thus, the surplus 3PLLA formed a small amount of microcrystallites. And the DSC measurement was not sensitive enough to detect the minor homochiral microcrystallites formed in that blend.

3. Blends of 3PLLA/3PDLA and 3PLLA/PDLA with Similar Molecular Weights. The DSC profiles of 3PLLA/3PDLA with similar molecular weights blends are displayed in Figure 7a, and the data collected from DSC are listed in Table 2. The T_{sc} increased first and then decreased as the molecular weight of 3PLAs increased from 9 to 100 kg/mol. The highest T_{sc} (232.1 °C) was found when both the molecular weights of 3PLAs were ca. 35 kg/mol. The fusion enthalpy of racemic crystallites (ΔH_{sc}) decreased consecutively, and their melt process became wider as increasing the molecular weight of PLAs in the blends, which suggested fewer crystallites, and higher lattice disorderness of racemic crystallites were formed in these specimens. Homochiral crystallites were observed when the molecular weights of the 3PLAs were around 100 kg/mol, which could be ascribed to the chain entanglement and viscosity being aggravated for such a high molecular weight. Thus, the stereocomplexation of racemic crystallites was imperfect; parts of the chain were not involved in complexation and generated homochiral crystallites.

dx.doi.org/10.1021/jp303402j | J. Phys. Chem. B 2012, 116, 9983−9991

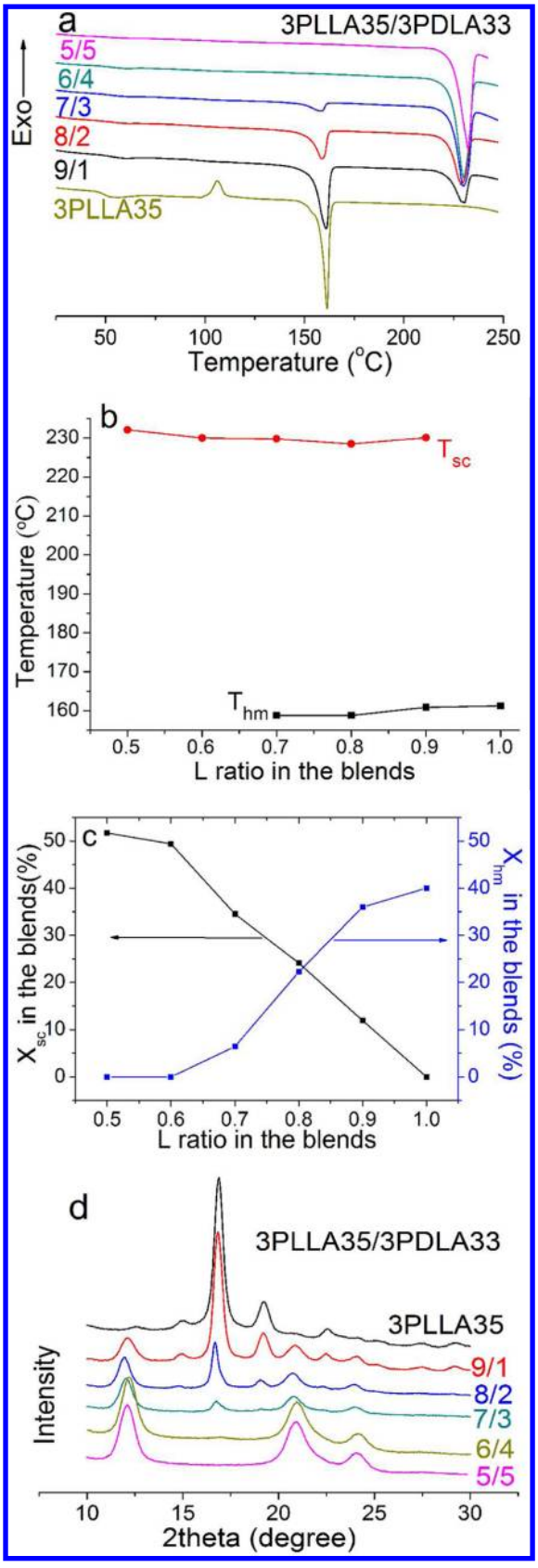

Figure 6. (a) DSC curves of 3PLLA35/3PDLA33 with different L/D ratios. (b) T_{hm} and T_{sc} of the 3PLLA35/3PDLA33 different L/D ratio blends. (c) X_{hm} and X_{sc} of these blends. (d) WAXD profile of these blends.

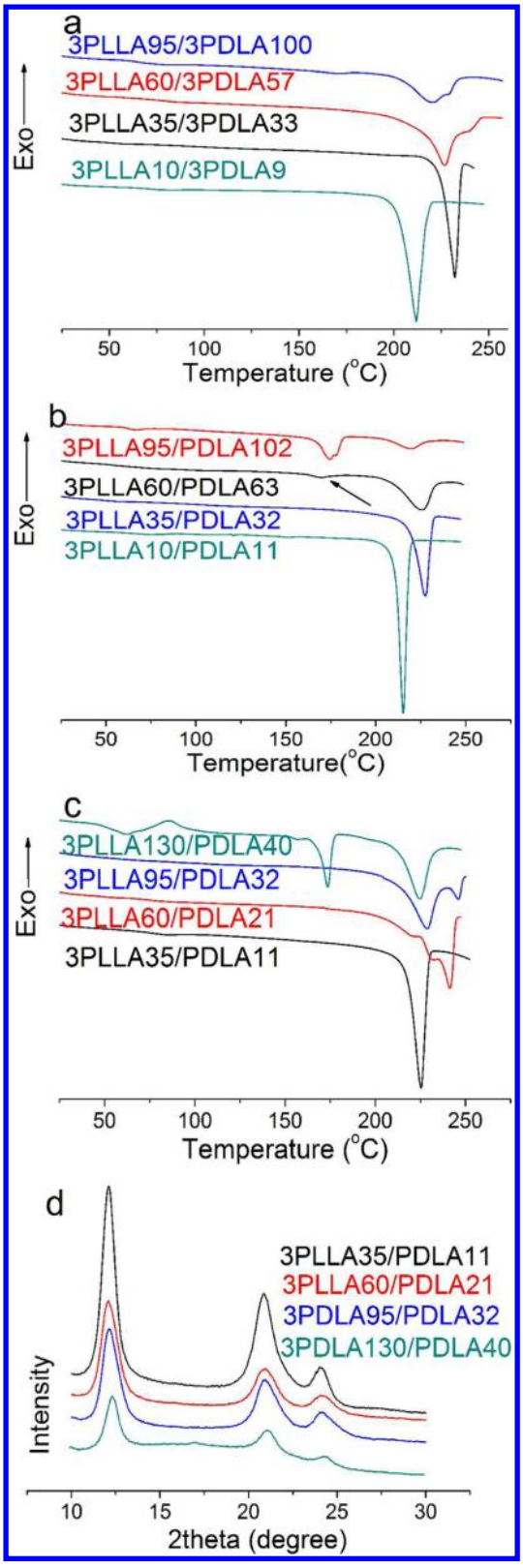

Figure 7. (a) DSC profile of 3PLLA/3PDLA with similar molecular weight. (b) DSC profile of 3PLLA/PDLA with similar molecular weight. (c) DSC thermogram of 3PLLA/PDLA blends, in which the molecular weight of PDLA was similar to the branch of 3PLLA. (d) WAXD of the blends in (c).

The DSC thermograms of 3PLLA/PDLA with similar molecular weights are exhibited in Figure 7b; the T_{sc} and X_{sc}

dx.doi.org/10.1021/jp303402j | J. Phys. Chem. B 2012, 116, 9983−9991

Table 2. Data of 3PLLA/3PDLA and 3PLLA/PDLA with Similar Molecular Weight Blends

specimens	T_{hm} (°C)	ΔH_{hm} (J/g)	T_{sc} (°C)	ΔH_{sc} (J/g)
3PLLA10/3PDLA9			211.8	80.6
3PLLA35/3PDLA33			232.1	73.4
3PLLA60/3PDLA57			226.5	71.6
3PLLA95/3PDLA100	170.7	2.6	220.7	46.2
3PLLA10/PDLA11			215.3	85.1
3PLLA35/PDLA32			227.6	68.2
3PLLA60/PDLA63	170.1	4.2	225.1	47.1
3PDLA95/PDLA102	174.8, 178.0	29.9	219.6	16.7
3PLLA35/PDLA11			225.3	82.2
3PLLA60/PDLA21			241.3[a]	78.2
3PLLA95/PDLA32			228.8[b]	72.1
3PLLA130/PDLA40[c]	173.7	20.8	224.6	41.8

[a]Mutimelt peak was observed during the DSC measurement, and 241.3 °C was the major melt peak. [b]228.8 °C was the major melt peak during the DSC scanning, and there was another peak at 246 °C. [c]There was an exothermic peak around the 85 °C, and we did not detracted the enthalpy during calculation.

revealed the analogous regularities to the 3PLLA/3PDLA blends in Figure 7a. However, homochiral crystallites were observed when both the molecular weight of 3PLLA and PDLA were ca. 60 kg/mol. The fusing enthalpy of homocrystallites (ΔH_{hm}) increased and the ΔH_{sc} decreased with increasing molecular weight of PLAs (the data collected form DSC measurements showed in Table 2). In addition, it was found that the T_{sc} and ΔH_{sc} shown in Figure 7b were slightly lower than Figure 7a, except 3PLLA10/PDLA11. These divergences could be ascribed to the dramatically different architecture between 3PLLA and PDLA, and the PDLA chain cannot complex with the branch of 3PLLA efficiently, especially, in high molecular weight blends.

When the molecular weight of linear PDLA was equal to the branch of 3PLLA, the DSC results of their blends are depicted in Figure 5c. For the blend of 3PLLA35/PDLA11, only a narrow melting peak at 225 °C was found, and the complexation was efficient because of high mobility of 3PLLA35 and PDLA11. When the molecular weights of PDLA and the branch of 3PLLA increased, the fusion of the stereocomplex crystallites became wide, and more than one melt peak were observed during heating. These implied the formed stereocomplexes was not uniform during solution evaporation, or melting recrystallization took place during heating. However, it was notable to see that the highest T_{sc} reached to 246 °C for the 3PLLA95/PDLA32 blend, which was the highest reported T_{sc} until now, although it was not a typical single melting process. An obvious exothermic peak and a melt endothermic peak around 170 °C were observed during DSC measurement in 3PLLA130/PDLA40, which indicated the crystallization was not adequate and homocrystallites were formed in that blend. The WAXD of these blends (Figure 7d) elaborated the intensity of racemic crystallites diffraction peaks receded, and the peaks turned broad as the molecular weight increased. The diffraction peak at 16.8° ascribed to PLA homochiral crystallites was detected in 3PLLA130/PDLA40. All illustrated that the formation of the stereocomplex crystalline in these blends getting arduous when the molecular weight of PDLA (or the branch of 3PLLA) enlarged from 11 to 40 kg/mol. The remarkable differences between DSC and WAXD profile of the 3PLLA130/PDLA40 were due to cold crystallization during heating.

The reasons for the variations of the T_{sc} and X_{sc} of these blends were just like above-mentioned (subsection 1.2); the higher T_{sc} of the blends was found in the middle molecular weights (e.g., 3PLLA35/PDLA32, 3PLLA35/3PDLA33, and 3PLLA95/PDLA32). If the molecular weights of the PLA or 3PLA continued increasing, the viscosity of the solution was heightened rapidly, and the PLA chain cannot interdiffuse and complex with enantiomers easily, especially to 3PLA for such compact structure. But they could discharge into the lattice by slightly adjustment and form homocrystallites. We called the formation of homochiral crystallites as phase separation—as the literature stated, microscopic phase separation.[9]

The different architectures of polymers exhibit different phase behaviors. In the linear PLLA/PDLA blends, the phase separation was detected when the molecular weight was ca. 60 kg/mol.[8] In our study, the phase separation for 3PLLA/3PDLA blends was observed when the molecular weights were ca. 100 kg/mol; the total molecular weight was larger than linear PLA blends. Nevertheless, the molecular weight of each branch was ca. 33 kg/mol, which was lower than linear PDLA/PLLA blends. For the blends which molecular weight of PDLA was similar to the branch of 3PLLA, homochiral crystallites were observed when the molecular weight of PDLA or when the branch of 3PLLA was ca. 40 kg/mol, slightly larger than the 3PLLA/3PDLA blends, and lower than linear PLLA/PDLA blends. The phase-separated molecular weight decreased gradually as the 3PLA increasing in the blends ($M_{\text{linear/linear blends}} > M_{\text{linear/3-armed blends}} > M_{\text{3-armed/3-armed blends}}$). These results might due to the huge steric hindrance of 3PLA. The phase separation was observed when both of the molecular weight of 3PLLA and PDLA were ca. 60 kg/mol, which may ascribed to the asymmetry structure between 3PLLA and PDLA, and the molecular weight of PDLA63 was disproportionate notably to the branch of 3PLLA60. Thus, one PDLA chain could not complex three branch of 3PLLA effectively.

4. CONCLUSIONS

In this work, the PLA stereocomplexes were prepared through 3PLLA blended with linear and 3-armed isomers; different structure and composition of poly(lactide) in the blends showed different thermal properties and phase behaviors. Through our investigations, the following conclusions could be made.

1. Stereocomplex crystallites, whose melting temperature varied form 210 to 250 °C, were preferentially formed in all binary blends, regardless of their architecture, constitution, and molecular weight.

2. In 3PLLA35/PDLA dissimilar blends, only stereocomplexes were formed in the blends. As the molecular weight of PDLA increased from 8 to 102 kg/mol, the T_{sc} increased first, then decreased, but the X_{sc} decreased monotonously. The highest T_{sc} (230.7 °C) was observed when molecular weight of PDLA was similar to the branch of 3PLLA35. For the 3PLLA35/3PDLA asymmetric molecular weight blends, both the T_{sc} and X_{sc} of the blends increased at first and then decreased as the molecular weight of 3PDLA increasing from 9 to 100 kg/mol. The T_{sc} and X_{sc} were highest when the molecular weights of 3PLAs were ca. 35 kg/mol.

3. In 3PLLA35/PDLA32 different L ratio blends, the T_{sc} and X_{sc} increased with the L ratio depressing from 1 to 0.5 in the blends. The situations of homochiral crystallites were just the

dx.doi.org/10.1021/jp303402j | J. Phys. Chem. B 2012, 116, 9983−9991

opposite. The 3PLLA35/3PDLA33 different ratio blends showed similar regularities as well as slight differences.

4. For similar molecular weight blends (or the linear PLA was similar to each branch of 3PLA enantiomers), higher T_{sc} of the blends were found in the middle molecular weights (3PLLA35/PDLA32, 3PLLA35/3PDLA33, and 3PLLA95/PDLA32). The highest T_{sc} reached 246 °C, which was the highest T_{sc} until now, although it was not a typical single melting process during DSC scanning. With the composition of 3PLA increasing, the phase separation molecular weight decreased gradually ($M_{linear/linear\ blends} > M_{linear/3\text{-}armed\ blends} > M_{3\text{-}armed/3\text{-}armed\ blends}$).

Through these studies, it could provide guidance for multiarmed PLA blending with their multiarmed or linear enantiomers and supply bases for their applications.

AUTHOR INFORMATION

Corresponding Author

*E-mail ligao@ciac.jl.cn, Fax +86-0431-85262667 (G.L.); e-mail xschen@ciac.jl.cn, Fax +86-0431-85262112 (X.C.).

Notes

The authors declare no competing financial interest.

ACKNOWLEDGMENTS

This work was supported by grants from National Natural Science Foundation of China (Projects 51073154, 51073155, 51033003 and 21004066), Ministry of Science and Technology of China (2011AA02A202), and Innovative Research Group (Project 51021003). All the authors appreciated help from the Dr. Jiangxun Ding and Dr. Chunsheng Xiao from CIAC.

REFERENCES

(1) Madhavan Nampoothiri, K.; Nair, N. R.; John, R. P. *Bioresour. Technol.* **2010**, *101*, 8493−8501.
(2) Sawyer, D. J. *Macromol. Symp.* **2003**, *201*, 271−281.
(3) Tokiwa, Y.; Jarerat, A. *Macromol. Symp.* **2003**, *201*, 283−289.
(4) Drumright, R. E.; Gruber, P. R.; Henton, D. E. *Adv. Mater.* **2000**, *12*, 1841−1846.
(5) Dorgan, J. R.; Lehermeier, H.; Mang, M. *J. Polym. Environ.* **2000**, *8*, 1−9.
(6) Pang, X.; Zhuang, X. L.; Tang, Z. H.; Chen, X. S. *Biotechnol. J.* **2010**, *5*, 1125−1136.
(7) Ikada, Y.; Jamshidi, K.; Tsuji, H.; Hyon, S. H. *Macromolecules* **1987**, *20*, 904−906.
(8) Tsuji, H.; Hyon, S. H.; Ikada, Y. *Macromolecules* **1991**, *24*, 5651−5656.
(9) Tsuji, H.; Hyon, S. H.; Ikada, Y. *Macromolecules* **1991**, *24*, 5657−5662.
(10) Tsuji, H.; Ikada, Y. *Macromolecules* **1992**, *25*, 5719−5723.
(11) Tsuji, H.; Ikada, Y. *Macromolecules* **1993**, *26*, 6918−6926.
(12) Tsuji, H. *Macromol. Biosci.* **2005**, *5*, 569−597.
(13) Fujita, M.; Sawayanagi, T.; Abe, H.; Tanaka, T.; Iwata, T.; Ito, K.; Fujisawa, T.; Maeda, M. *Macromolecules* **2008**, *41*, 2852−2858.
(14) He, Y.; Xu, Y.; Wei, J.; Fan, Z. Y.; Li, S. M. *Polymer* **2008**, *49*, 5670−5675.
(15) Yamane, H.; Sasai, K. *Polymer* **2003**, *44*, 2569−2575.
(16) Tsuji, H.; Takai, H.; Saha, S. K. *Polymer* **2006**, *47*, 3826−3837.
(17) Urayama, H.; Kanamori, T.; Fukushima, K.; Kimura, Y. *Polymer* **2003**, *44*, 5635−5641.
(18) Tsuji, H.; Yamamoto, S. *Macromol. Mater. Eng.* **2011**, *296*, 583−589.
(19) Purnama, P.; Kim, S. H. *Macromolecules* **2010**, *43*, 1137−1142.
(20) Chang, L.; Woo, E. M. *Macromol. Chem. Phys.* **2011**, *212*, 125−133.
(21) Tsuji, H.; Bouapao, L. *Polym. Int.* **2012**, *61*, 442−450.
(22) Nurkhamidah, S.; Woo, E. M. *Macromol. Chem. Phys.* **2011**, *212*, 1663−1670.
(23) Sun, J.; Yu, H.; Zhuang, X.; Chen, X.; Jing, X. *J. Phys. Chem. B* **2011**, *115*, 2864−2869.
(24) Wang, X.; Prud'homme, R. E. *Macromol. Chem. Phys.* **2011**, *212*, 691−698.
(25) Bouapao, L.; Tsuji, H. *Macromol. Chem. Phys.* **2009**, *210*, 993−1002.
(26) Rathi, S.; Chen, X.; Coughlin, E. B.; Hsu, S. L.; Golub, C. S.; Tzivanis, M. J. *Polymer* **2011**, *52*, 4184−4188.
(27) Brochu, S.; Prudhomme, R. E.; Barakat, I.; Jerome, R. *Macromolecules* **1995**, *28*, 5230−5239.
(28) Narladkar, A.; Balnois, E.; Grohens, Y. *Macromol. Symp.* **2006**, *241*, 34−44.
(29) Kondo, K.; Kida, T.; Ogawa, Y.; Arikawa, Y.; Akashi, M. *J. Am. Chem. Soc.* **2010**, *132*, 8236−8237.
(30) Tsuji, H.; Wada, T.; Sakamoto, Y.; Sugiura, Y. *Polymer* **2010**, *51*, 4937−4947.
(31) Masutani, K.; Kawabata, S.; Aoki, T.; Kimura, Y. *Polym. Int.* **2010**, *59*, 1526−1530.
(32) Hirata, M.; Kimura, Y. *Polymer* **2008**, *49*, 2656−2661.
(33) Kakuta, M.; Hirata, M.; Kimura, Y. *Polym. Rev.* **2009**, *49*, 107−140.
(34) Yui, N.; Dijkstra, P. J.; Feijen, J. *Makromol. Chem.* **1990**, *191*, 481−488.
(35) Hirata, M.; Kobayashi, K.; Kimura, Y. *J. Polym. Sci., Polym. Chem.* **2010**, *48*, 794−801.
(36) Stevels, W. M.; Ankone, M. J. K.; Dijkstra, P. J.; Feijen, J. *Macromol. Chem. Phys.* **1995**, *196*, 3687−3694.
(37) Zhang, Z.; Grijpma, D. W.; Feijen, J. *Macromol. Chem. Phys.* **2004**, *205*, 867−875.
(38) Kricheldorf, H. R.; Rost, S.; Wutz, C.; Domb, A. *Macromolecules* **2005**, *38*, 7018−7025.
(39) Li, L. B.; Zhong, Z. Y.; de Jeu, W. H.; Dijkstra, P. J.; Feijen, J. *Macromolecules* **2004**, *37*, 8641−8646.
(40) Fukushima, K.; Hirata, M.; Kimura, Y. *Macromolecules* **2007**, *40*, 3049−3055.
(41) Hirao, A.; Yoo, H.-S. *Polym. J.* **2011**, *43*, 2−17.
(42) Liu, H.; Zhang, J. *J. Polym. Sci., Polym. Phys.* **2011**, *49*, 1051−1083.
(43) Zhu, X.; Zhou, Y.; Yan, D. *J. Polym. Sci., Polym. Phys.* **2011**, *49*, 1277−1286.
(44) Biela, T.; Duda, A.; Pasch, H.; Rode, K. *J. Polym. Sci., Polym. Phys. Chem.* **2005**, *43*, 6116−6133.
(45) Biela, T.; Duda, A.; Penczek, S.; Rode, K.; Pasch, H. *J. Polym. Sci., Polym. Phys. Chem.* **2002**, *40*, 2884−2887.
(46) Biela, T.; Duda, A.; Rode, K.; Pasch, H. *Polymer* **2003**, *44*, 1851−1860.
(47) Biela, T.; Polanczyk, I. *J. Polym. Sci., Polym. Phys. Chem.* **2006**, *44*, 4214−4221.
(48) Biela, T. *Polimery* **2007**, *52*, 106−116.
(49) Biela, T.; Duda, A.; Penczek, S. *Macromolecules* **2006**, *39*, 3710−3713.
(50) Nagahama, K.; Fujiura, K.; Enami, S.; Ouchi, T.; Ohya. *J. Polym. Sci., Polym. Phys. Chem.* **2008**, *46*, 6317−6332.
(51) Nagahama, K.; Nishimura, Y.; Ohya, Y.; Ouchi, T. *Polymer* **2007**, *48*, 2649−2658.
(52) Tsuji, H.; Miyase, T.; Tezuka, Y.; Saha, S. K. *Biomacromolecules* **2005**, *6*, 244−254.
(53) Hao, Q. H.; Li, F. X.; Li, Q. B.; Li, Y.; Jia, L.; Yang, J.; Fang, Q.; Cao, A. M. *Biomacromolecules* **2005**, *6*, 2236−2247.
(54) Lee, C. W.; Kimura, Y. *Bull. Chem. Soc. Jpn.* **1996**, *69*, 1787−1795.
(55) Loomis, G. L.; Murdoch, J. R.; Gardner, K. H. *Polym. Prepr.* **1990**, *200*, 55.
(56) Fischer, E. W.; Sterzel, H. J.; Wegner, G. *Colloid Polym. Sci.* **1973**, *251*, 980−990.
(57) Okihara, T.; Tsuji, M.; Kawaguchi, A.; Katayama, K.; Tsuji, H.; Hyon, S. H.; Ikada, Y. *J. Macromol. Sci., Phys.* **1991**, *B30*, 119−140.

(58) Brizzolara, D.; Cantow, H. J.; Diederichs, K.; Keller, E.; Domb, A. J. *Macromolecules* **1996**, *29*, 191−197.
(59) Bouapao, L.; Tsuji, H.; Tashiro, K.; Zhang, J.; Hanesaka, M. *Polymer* **2009**, *50*, 4007−4017.
(60) Kawai, T.; Rahman, N.; Matsuba, G.; Nishida, K.; Kanaya, T.; Nakano, M.; Okamoto, H.; Kawada, J.; Usuki, A.; Honma, N.; Nakajima, K.; Matsuda, M. *Macromolecules* **2007**, *40*, 9463−9469.
(61) Kang, N.; Perron, M. E.; Prud'homme, R. E.; Zhang, Y. B.; Gaucher, G.; Leroux, J. C. *Nano Lett.* **2005**, *5*, 315−319.